Paweł JABŁOŃSKI

Częstochowa University of Technology

Cylindrical conductor in an arbitrary time-harmonic transverse magnetic field

Abstract. *A long cylindrical conductor in an arbitrary time-harmonic transverse magnetic field is considered in the paper. The source magnetic vector potential near the conductor is expressed as power series in the cylindrical coordinates. By using the method of separation of variables, the magnetic field inside and outside the conductor as well as the eddy currents and Joule's power losses were determined. The dependency of Joule's power losses due to n-th spatial harmonic was investigated as a function of various parameters.*

Streszczenie. *Rozważono długi cylindryczny przewodnik w dowolnym poprzecznym harmonicznym polu magnetycznym. Potencjał wektorowy źródłowego pola magnetycznego przedstawiono w postaci szeregu potęgowego i metodą rozdzielania zmiennych określono pole magnetyczne, prądy wirowe oraz straty mocy. Przeanalizowano zależność strat mocy od n-tej harmonicznej przestrzennej w funkcji różnych parametrów. (**Długi cylindryczny przewodnik w dowolnym poprzecznym harmonicznym polu magnetycznym**)*

Keywords: time-harmonic magnetic field, eddy currents, power losses, cylindrical conductor.
Słowa kluczowe: harmoniczne pole magnetyczne, prądy wirowe, straty mocy, przewodnik cylindryczny.

Introduction

Infinitely long, straight conductors of constant cross-section are often models of many real configurations with electromagnetic field, e.g. power lines, transmission lines, material samples in induction heating. Such configurations have been widely discussed in literature, e.g. [1-5]. This paper is a generalization of the considerations from [1-3], which concern an infinitely long, straight wire of circular cross-section exposed to an external, time-harmonic magnetic field generated by a current in another parallel wire. To find out the eddy currents in the first wire, a power series expansion of the magnetic vector potential due to the second wire was used there. This approach is generalized here by considering an external transverse magnetic field to have the form of power series with coefficients, whose values depend on the configuration of source currents. By using the method of separation of variables, the magnetic field inside and outside the conductor as well as eddy currents and power losses were determined. The dependency of power losses due to n-th spatial harmonic was investigated as a function of various parameters.

Problem description

A long conductor of circular cross-section of radius a is located along z axis of cylindrical coordinates in a non-conducting region, and exposed to a time harmonic transverse magnetic field generated by other long conductors parallel to the considered one (see Fig. 1).

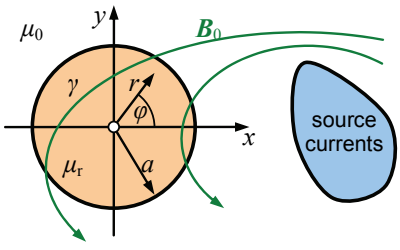

Fig.1. Long cylindrical conductor in a transverse magnetic field

The goal is to determine eddy currents induced in the conductor by the field and power losses due to them. To achieve it the following simplifications and assumptions were done:

- all conductors are infinitely long,
- the field is independent on z coordinate,
- the currents in source regions generate time-harmonic magnetic field of angular frequency ω,
- conductivity, γ, and relative permeability, μ_r, of the considered conductor are constant,
- the reverse reaction on the source conductors can be neglected.

Due to the first two assumptions the problem may be regarded as a 2D one, in which the magnetic vector potential has a z-component only, which is independent of z coordinate, i.e.

$$\underline{\boldsymbol{A}} = \underline{A}(r,\varphi)\boldsymbol{1}_z \,, \tag{1}$$

where $\boldsymbol{1}_z$ is a unit vector of z axis, r, φ – polar coordinates. The source vector magnetic potential (its z-component) in the vicinity of the conductor is assumed to have the form

$$\underline{A}_0(r,\varphi) = \underline{B}_0 a \sum_{n=1}^{\infty} C_{0n}\left(\frac{r}{a}\right)^n \operatorname{trig} n\varphi \,, \tag{2}$$

where: B_0 - magnetic flux density, a – conductor's radius, C_{0n} – dimensionless constants, and

$$\operatorname{trig} n\varphi = c_n \cos n\varphi + s_n \sin n\varphi \,, \tag{3}$$

where c_n and s_n are normalized constants ($c_n c_n^* + s_n s_n^* = 1$). Series (2) is assumed to be converge in a ring $a \le r < r_0$.

Magnetic field and eddy currents in the conductor

Inside the cylindrical conductor ($r \le a$), the z-component of magnetic vector potential satisfies Helmholtz's equation

$$\nabla^2 \underline{A}_{\text{int}} - \underline{k}^2 \underline{A}_{\text{int}} = 0 \,, \tag{4}$$

where

$$\underline{k}^2 = \mathrm{j}\omega\mu_r\mu_0\gamma \,, \tag{5}$$

$$\underline{k} = \frac{1}{\delta} + \mathrm{j}\frac{1}{\delta}, \qquad \delta = \sqrt{\frac{2}{\omega\mu_r\mu_0\gamma}} \,, \tag{6}$$

with δ as the skin depth. By using the method of separation of variables the solution of Eq. (4) becomes

$$\underline{A}_{\text{int}}(r,\varphi) = \sum_{n=0}^{\infty} [C_{1n} I_n(\underline{k}r) + D_{1n} K_n(\underline{k}r)] \operatorname{trig} n\varphi \,, \tag{7}$$

where C_{1n} and D_{1n} are constants to be found, I_n and K_n – modified Bessel functions of order n of the first and second kind, respectively. To obtain finite values of $\underline{A}_{\text{int}}$ for $r = 0$ the term with K_n should be discarded, because when $r \to 0$, $K_n(\underline{k}r)$ tends to infinity. Thus $D_{1n} = 0$.

In the vicinity of the conductor, outside the region with source currents, magnetic vector potential (its z-component) satisfies the Laplace equation

$$\nabla^2 \underline{A}_{\text{ext}} = 0 . \tag{8}$$

Its solution has the form

$$\underline{A}_{\text{ext}} = \underline{A}_0 + \underline{A}_2 , \tag{9}$$

where $\underline{A}_0$ is the source potential (2), and $\underline{A}_2$ is an adjustment due to the presence of the conductor, equal

$$\underline{A}_2 = C_{20} + D_{20} \ln r + \sum_{n=1}^{\infty} (C_{2n} r^n + D_{2n} r^{-n}) \operatorname{trig} n\varphi , \tag{10}$$

where C_{2n} and D_{2n} are constants to be determined. $\underline{A}_{\text{ext}}$ should tend to $\underline{A}_0$ for large r, hence $\underline{A}_2$ should vanish then, from which it follows that $D_{20} = C_{2n} = 0$.

Constants C_{1n} in Eq. (7) and D_{2n} in (10) are determined by the continuity conditions for electromagnetic field on the cylinder's surface ($r = a$), i.e.

$$\underline{A}_{\text{int}} = \underline{A}_{\text{ext}}, \qquad \frac{1}{\mu_{\text{r}}} \frac{\partial \underline{A}_{\text{int}}}{\partial r} = \frac{\partial \underline{A}_{\text{ext}}}{\partial r} . \tag{11}$$

The conditions lead to the following equations:

$$\begin{cases} C_{10} I_0(\underline{\kappa}) = C_{20}, \\ \dfrac{1}{\mu_{\text{r}}} C_{10} \underline{k} I_0'(\underline{\kappa}) = 0, \end{cases} \tag{12}$$

for $n = 0$, and

$$\begin{cases} C_{1n} I_n(\underline{\kappa}) = \underline{B}_0 a C_{0n} + D_{2n} a^{-n}, \\ \dfrac{1}{\mu_{\text{r}}} C_{1n} \underline{k} I_n'(\underline{\kappa}) = n \underline{B}_0 C_{0n} - D_{2n} n a^{-n-1}, \end{cases} \tag{13}$$

for $n > 0$, where

$$\underline{\kappa} = \underline{k} a = \frac{a}{\delta} + \mathrm{j}\frac{a}{\delta} = \alpha + \mathrm{j}\alpha, \qquad \alpha = \frac{a}{\delta} . \tag{14}$$

Hence, $C_{10} = C_{20} = 0$, and

$$\begin{cases} C_{1n} = \underline{B}_0 a C_{0n} M_n \dfrac{1}{I_n(\underline{\kappa})}, \\ D_{2n} = \underline{B}_0 a C_{0n} (M_n - 1) a^n, \end{cases} \tag{15}$$

where

$$M_n = M_n(\mu_{\text{r}}, \underline{\kappa}) = \frac{2\mu_{\text{r}}}{\mu_{\text{r}} + \widetilde{I}_n(\underline{\kappa})} , \tag{16}$$

with an auxiliary function defined as

$$\widetilde{I}_n(z) = \frac{z I_n'(z)}{n I_n(z)} . \tag{17}$$

Taking into account the above expressions, the vector magnetic potential can be expressed as:

$$\underline{A}_{\text{int}} = \underline{B}_0 a \sum_{n=1}^{\infty} C_{0n} M_n \frac{I_n\left(\underline{\kappa}\dfrac{r}{a}\right)}{I_n(\underline{\kappa})} \operatorname{trig} n\varphi , \tag{18}$$

$$\underline{A}_{\text{ext}} = A_0 + \underline{B}_0 a \sum_{n=1}^{\infty} C_{0n} (M_n - 1) \left(\frac{a}{r}\right)^n \operatorname{trig} n\varphi . \tag{19}$$

Density of eddy currents induced in the conductor, $\underline{J}_{\text{int}}$, can be expressed as $-\mathrm{j}\omega\gamma\underline{A}_{\text{int}}$, which yields

$$\underline{J}_{\text{int}} = -\frac{\underline{B}_0}{\mu_0 a} \frac{\underline{\kappa}^2}{\mu_{\text{r}}} \sum_{n=1}^{\infty} C_{0n} M_n \frac{I_n\left(\underline{\kappa}\dfrac{r}{a}\right)}{I_n(\underline{\kappa})} \operatorname{trig} n\varphi . \tag{20}$$

Magnetic flux density, $\underline{\boldsymbol{B}}$, can be found as $\operatorname{curl}\underline{\boldsymbol{A}}$, from which it follows that inside the conductor

$$\underline{B}_{\text{int}\,r} = \underline{B}_0 \sum_{n=1}^{\infty} C_{0n} M_n n \frac{a}{r} \frac{I_n\left(\underline{\kappa}\dfrac{r}{a}\right)}{I_n(\underline{\kappa})} \operatorname{trig}' n\varphi , \tag{21}$$

$$\underline{B}_{\text{int}\,\varphi} = \underline{B}_0 \sum_{n=1}^{\infty} C_{0n} M_n \underline{\kappa} \frac{I_n'\left(\underline{\kappa}\dfrac{r}{a}\right)}{I_n(\underline{\kappa})} \operatorname{trig} n\varphi . \tag{22}$$

Similar formulas express the magnetic flux density outside the conductor.

Joule's power losses

Apparent power supplied to the conductor can be found as the Poynting vector flux through the surface of the cylindrical conductor. Apparent power $\underline{S}'$ per unit of length of the conductor can be expressed as

$$\underline{S}' = \frac{\mathrm{j}\omega}{\mu_0 \mu_{\text{r}}} \int_0^{2\pi} \left(\underline{A}_{\text{int}} \frac{\partial \underline{A}_{\text{int}}^*}{\partial r} \right)_{r=a} a \, \mathrm{d}\varphi . \tag{23}$$

Putting Eq. (18) into the above formula, performing the integration yields

$$\underline{S}' = \frac{B_0^2 \pi}{\gamma \mu_0^2} \frac{\underline{\kappa}^2}{\mu_{\text{r}}^2} \sum_{n=1}^{\infty} n \left| C_{0n} \right|^2 M_n M_n^* \widetilde{I}_n^*(\underline{\kappa}) . \tag{24}$$

The real part of this expression determines power losses in the conductor per unit of length. It can be written as

$$P' = \operatorname{Re} \underline{S}' = \sum_{n=1}^{\infty} \left| C_{0n} \right|^2 P_n' , \tag{25}$$

where

$$P_n' = B_0^2 \frac{\pi}{\gamma \mu_0^2} p_n(\alpha, \mu_{\text{r}}) , \tag{26}$$

$$p_n(\alpha, \mu_{\text{r}}) = \frac{8 n \alpha^2}{\left| \mu_{\text{r}} + \widetilde{I}_n(\alpha + \mathrm{j}\alpha) \right|^2} \operatorname{Im}[\widetilde{I}_n(\alpha + \mathrm{j}\alpha)] , \tag{27}$$

with $\alpha = a/\delta$ – see Eq. (14). Dimensionless function $p_n(\alpha, \mu_{\text{r}})$ is the contribution of n-th spatial harmonic into Joule's power losses. Figures 2 and 3 present $p_n \alpha^{-4}$ as a function of α for different values of n and μ_{r}.

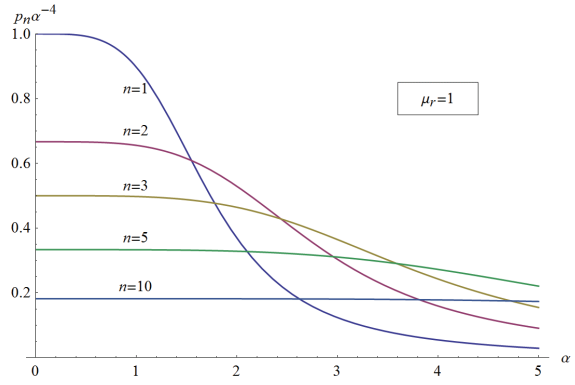

Fig.2. Changes in $p_n\alpha^{-4}$ versus α for different values of n at μ_r = 1

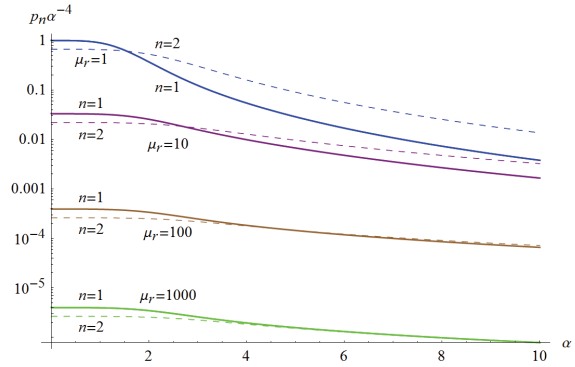

Fig.3. Changes in $p_n\alpha^{-4}$ versus α for different values of μ_r and n

The contribution p_n for small values of α is highest for n = 1, and decreases if n increases. For α large enough, the greater is n the greater is the contribution p_n. Figure 3 suggest that p_n is much smaller for magnetic cylinder than for non-magnetic one. However, it should be taken into account that α depends on μ_r. Therefore, it is worth to compare the values of p_n versus frequency for magnetic and non-magnetic cylinders of the same conductivity and dimensions. To achieve it, let us express α as

$$\alpha = \sqrt{\frac{f\mu_r}{f_0}}, \qquad f_0 = \frac{1}{\pi\mu_0\gamma a^2}. \tag{28}$$

Frequency f_0 is a reference frequency, at which the skin depth δ for a non-magnetic cylinder equals the radius a of the cylinder's cross-section. Figure 4 shows changes in p_n versus frequency f for different values of n and μ_r. Power losses for low frequencies are greater in magnetic conductor, but there is a range of frequency in which the contrary relation takes place.

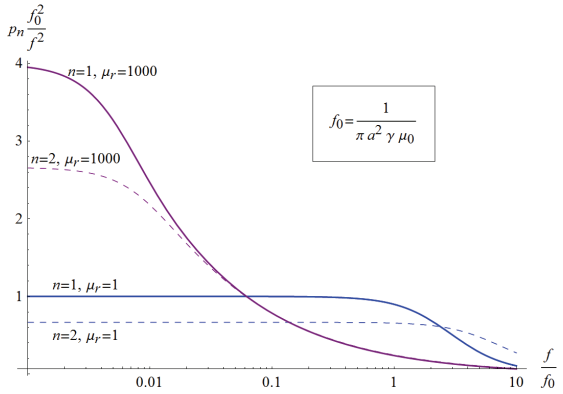

Fig.4. Changes in $(f/f_0)^{-2}p_n$ versus f/f_0 for different values of μ_r and n

Figure 5 shows how the power losses P'_n depend on the radius of the cylinder at a constant frequency of 50 Hz. Three materials were taken into account: copper (γ = $5.8\cdot10^7$ S·m^{-1}, μ_r = 1), aluminum (γ = $3.63\cdot10^7$ S·m^{-1}, μ_r = 1) and iron (γ = $1.03\cdot10^7$ S·m^{-1}, μ_r assumed to be 1000).

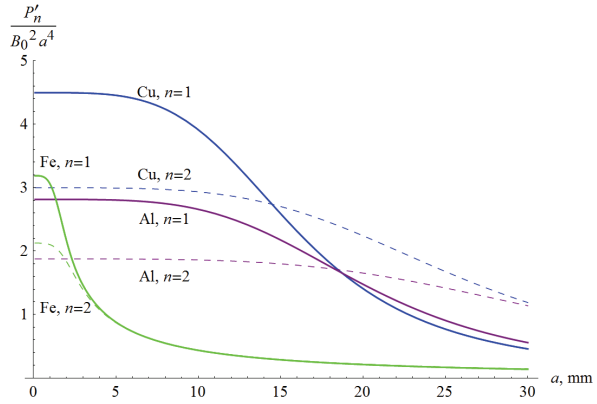

Fig. 5. Changes in $P'_nB_0^{-2}a^{-4}$ versus a in cylinders made of copper, aluminum and iron (at μ_r = 1000) for two lowest spatial harmonics at a constant frequency of 50 Hz (a given in mm, B_0 in T).

Although formulas (25)-(27) describe exactly how power losses depend on different parameters, it is worth to analyze them in special cases. Let us begin from the case α << 1, which corresponds to low frequencies f << f_0/μ_r. Expanding (27) into power series and preserving the term of the lowest order in α, yields

$$p_n \approx \frac{8\alpha^4}{(n+1)(\mu_r+1)^2} = \frac{8}{n+1}\left(\frac{\mu_r}{\mu_r+1}\right)^2\left(\frac{f}{f_0}\right)^2. \tag{29}$$

Thus, for low frequencies the value of p_n is proportional to the square of frequency and inversely proportional to the number of spatial harmonic. Using the above result in (26), we obtain

$$P'_n \approx B_0^2\frac{8\pi^3}{n+1}\left(\frac{\mu_r}{\mu_r+1}\right)^2\gamma a^4 f^2. \tag{30}$$

Power losses due to n-th spatial harmonic at low frequencies are directly proportional to the conductivity of the conductor as well as to the fourth power of radius of the conductor. For non-magnetic cylinder (μ_r = 1) the above expression simplifies to

$$P'^{\mu_r=1}_n \approx B_0^2\frac{2\pi^3}{n+1}\gamma a^4 f^2, \tag{31}$$

while for magnetic (μ_r >> 1)

$$P'^{\mu_r>>1}_n \approx B_0^2\frac{8\pi^3}{n+1}\gamma a^4 f^2 = 4P'^{\mu_r=1}_n. \tag{32}$$

Compare the result obtained with Fig. 4, in which it is visible that p_n at very low frequencies is approximately four times greater for magnetic conductor than for non-magnetic one. It is worth noting that this approximation is quite good even for $\alpha \approx 1$ (i.e. $f \approx f_0/\mu_r$), because the coefficient at α^8 in the power series expansion of expression (27) is much less than the one at α^4. This is noticeable especially for n > 1 or μ_r >> 1.

To obtain approximate formulas for high frequency let us observe that for $|z|$ >> n it holds [6]

$$\tilde{I}_n(z) \approx \frac{z}{n}. \tag{33}$$

Thus, for α >> n, which corresponds to f >> $n^2 f_0/\mu_r$, formula (27) can approximated by

$$p_n \approx 8n^2 \frac{\alpha^3}{(n\mu_r+\alpha)^2+\alpha^2}. \tag{34}$$

If α >> $n\mu_r$, what is fulfilled for non-magnetic cylinder (or magnetic for very large α), the formula reduces to

$$p_n \approx 4n^2(\alpha - n\mu_r) = 4n^2\left(\sqrt{\mu_r \frac{f}{f_0}} - n\mu_r\right). \tag{35}$$

At μ_r = 1 it gives

$$P_n' \approx B_0^2 \frac{4\pi}{\mu_0} n^2 a\left(\sqrt{\frac{\pi f}{\mu_0 \gamma}} - n\right). \tag{36}$$

Power losses due to n-th spatial harmonic at high frequencies for non-magnetic cylinder are proportional to the square root of frequency, the square of harmonic number, the radius of the cylinder, and inversely proportional to the square root of conductivity.

Subsequently, if α << $n\mu_r$, what can occur only for a magnetic cylinder (because we assumed that α >> n), we obtain

$$p_n \approx 8\frac{\alpha^3}{\mu_r^2} = \frac{8}{\sqrt{\mu_r}}\left(\frac{f}{f_0}\right)^{\frac{3}{2}}, \tag{37}$$

$$P_n' \approx 8\pi^2 B_0^2 a^3 \sqrt{\frac{\pi\gamma}{\mu_0\mu_r}} f^{\frac{3}{2}}. \tag{38}$$

Thus, Joule's power losses due to n-th spatial harmonic for large enough frequency in magnetic cylinder are proportional to the third power of the square root of frequency, the third power of the radius of the cylinder, the square root of conductivity, and inversely proportional to the square root of permeability. It is worth noting that they do not depend on the number of harmonic.

Numerical example

Let the source of magnetic field is a long filament carrying time-harmonic current $\underline{I}$ (see Fig. 6). The distance between axes of filament and the considered cylinder equals d.

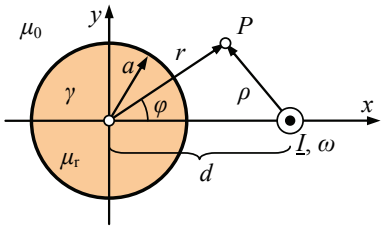

Fig. 6. Cylinder near a long filament carrying time-harmonic current

The z-component of the source vector magnetic potential at point P equals

$$\underline{A}_0 = \frac{\mu_0 \underline{I}}{2\pi} \ln\frac{1}{\rho} + C, \tag{39}$$

where ρ is the distance between point P and the filament, and C is a constant that can be freely assumed. Expressing distance ρ by r, d and φ yields

$$\underline{A}_0 = \frac{\mu_0 \underline{I}}{2\pi}\left[\ln\frac{1}{d} - \frac{1}{2}\ln\left(1+\left(\frac{r}{d}\right)^2 - 2\frac{r}{d}\cos\varphi\right)\right] + C. \tag{40}$$

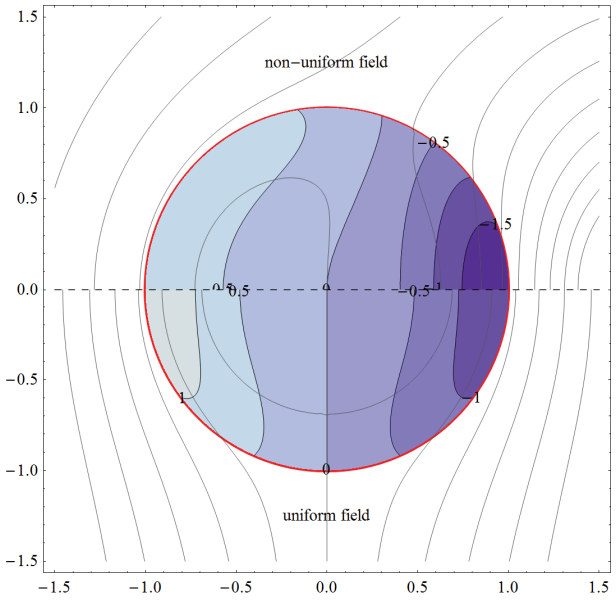

Fig.7. Lines of magnetic flux density (gray lines) and distribution of current density (20) (shaded contours) at a certain phase for d = 2a, α = 3, μ_r = 1; the upper part corresponds to the considered configuration while the lower to the first spatial harmonic (n = 1); values of current density are referred to $I/\pi a^2$; axes scaled in a.

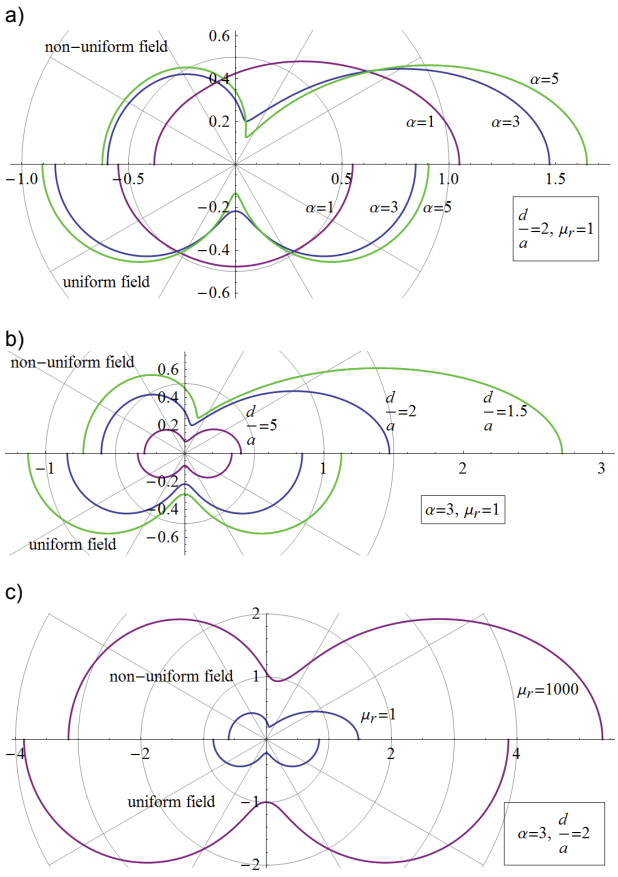

Fig.8. Distribution of the maximum value of magnetic flux density on the surface of the cylinder for different values of parameters: a) d = 2a, μ_r = 1, α = 1, 3, 5; b) α = 3, μ_r = 1, d = 1.5a, 2a, 5a; c) d = 2a, α = 3, μ_r = 1, 1000; the upper parts refer to the considered configuration, while the lower to the first spatial harmonic (n = 1); axes scaled in $\sqrt{2}B_0$.

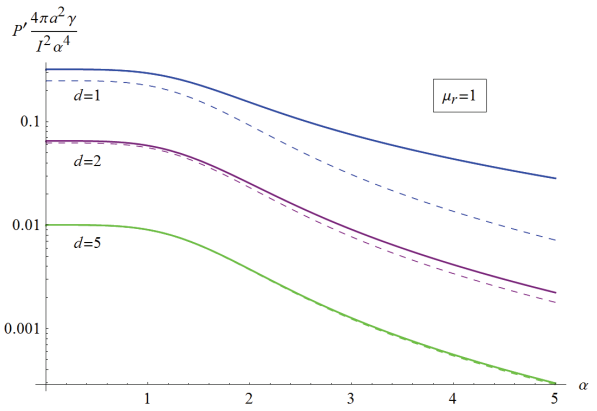

Fig.9. Power losses per unit length, P' (25), versus α for different values of distance d and μ_r = 1 (solid lines); dashed lines correspond to power losses due to the uniform magnetic field of the first spatial harmonic (n = 1); axis of P' scaled in $I^2\alpha^4/4\pi\gamma a^2$.

Using the following expansion (truthful for x < 1) [7]

$$\ln(1+x^2-2x\cos\varphi) = -2\sum_{n=1}^{\infty}\frac{1}{n}x^n\cos n\varphi\,, \tag{41}$$

leads us to

$$\underline{A}_0 = \frac{\mu_0 \underline{I}}{2\pi}\sum_{n=1}^{\infty}\frac{1}{n}\left(\frac{r}{d}\right)^n\cos n\varphi + \left(C - \frac{\mu_0 \underline{I}}{2\pi}\ln d\right), \tag{42}$$

which is truthful for r < d (i.e. the convergence radius r_0 = d). Comparing the result obtained with Eq. (2) allows us to identify that

$$\underline{B}_0 = \frac{\mu_0 \underline{I}}{2\pi a}, \quad C_{0n} = \frac{1}{n}\left(\frac{a}{d}\right)^n, \quad c_n = 1, \quad s_n = 0\,. \tag{43}$$

Figure 7 shows the lines of magnetic flux density and distribution of current density at a certain phase for arbitrary parameters. Figure 8 shows the distribution of the maximum value of magnetic flux density on the surface of the cylinder for different values of parameters. The upper parts of the figures correspond to the considered configuration, while the lower ones – to the uniform field due to the first spatial harmonic (n = 1). Figure 9 presents power losses P' as a function of α for different values of d/a and μ_r = 1.

Concluding remarks

Based on the above considerations the following conclusions can be formulated:

- for low frequency power losses are inversely proportional to the number of spatial harmonic of the source magnetic field; they are approximately four times greater in a magnetic material than in a non-magnetic one;
- for high frequency power losses are approximately proportional to the square of spatial harmonic number in a non-magnetic cylinder while are independent of the harmonic number in a magnetic one;
- for low frequency power losses are proportional to the square of frequency while for high frequency they are proportional to the square root of frequency in a non-magnetic cylinder and to the third power of the square root of the frequency in a magnetic one (which remains in accordance with known facts).

REFERENCES

[1] Piątek Z., Impedances of tubular high current busducts, Wydawnictwo Politechniki Częstochowskiej, *seria Postępy Techniki Wysokich Napięć*, tom 28, Częstochowa 2008.

[2] Piątek Z., Joule's Power losses in a cylindrical conductor caused by eddy currents induced by the current in the parallel conductor (in Polish), *ZN Pol. Śl., Elektryka*, 75 (1981), 151-157.

[3] Piątek Z., Method of calculating eddy currents induced by the sinusoidal current of the parallel conductor in the circular conductor, *ZN Pol. Śl., Elektryka*, 75 (1981), 137-150.

[4] Rolicz P., Eddy currents generated in a system of two cylindrical conductors by a transverse alternating magnetic field, *Electric Power Systems Research*, 79 (2009), 2, 295-300.

[5] Krakowski M., Szymański G., Numerical analysis of eddy-currents induced in a metal cylinder by AC in parallel conductor, *Archiwum Elektrotechniki*, XXVII (1978), 1, 133-142.

[6] McLachlan N.W., Bessel function for engineers (in Polish), PWN, Warsaw 1964.

[7] Gradsztejn I.S., Ryżyk I.M., Tables of integrals, sums, series and products (in Polish), PWN, Warsaw1972.

Author: *dr inż. Paweł Jabłoński, Politechnika Częstochowska, Wydział Elektryczny, al. Armii Krajowej 17, 42-200 Częstochowa, E-mail: paweljablonski7@gmail.com.*